ISBN: 978-3-95450-247-9 ISSN: 2673-5490 doi: 10.18429/JACoW-IPAC2024-MOPS33

SINGLE-BUNCH INSTABILITIES AND THEIR MITIGATION IN DIAMOND-II

D. Rabusov*, R.T. Fielder, S. Wang, I.P.S. Martin, Diamond Light Source, Oxfordshire, UK

Abstract

Diamond-II is a future 4-th generation synchrotron light source with a significantly narrower vacuum chamber compared to the existing Diamond storage ring. The strength of wake fields will increase, and, consequently, the risk of single-bunch instabilities also rises. We consider chromaticity adjustment and a passive harmonic cavity as mitigation measures, including for cases with impedance strength larger than the design value. This work presents single-bunch thresholds obtained in particle tracking simulations for the latest lattice and impedance database, including the case of non-equal bunch lengthening in realistic filling patterns due to beam loading in the RF cavities. The impedance database includes accurate computations of asymmetric vessels causing non-zero monopole and quadrupole components of the wake. Resulting emittance dilution due to impedance is found to be tolerable.

INTRODUCTION

Collective effects might limit the intensity of a 4th generation light source. In the case of Diamond-II, single-bunch instabilities caused by the interaction between electrons and vacuum chamber could lead to significant particle losses and poor beam quality [1] if not addressed. The most recent progress on the construction of the Diamond-II impedance database, used in this work, is presented in Ref. [2].

SINGLE-BUNCH INSTABILITY THRESHOLDS

Most results presented in this section have been obtained from particle-tracking simulations in Elegant [3]. The model consists of a one-turn map, wake potentials (elements *wake* and *trwake* for the geometric components), impedance elements (for the resistive-wall components) *zlongit* and two *ztransverse* elements, the RF cavity, the harmonic cavity (optional), and the *sreffects* element for synchrotron radiation. We use two transverse impedance elements (resistive wall) to resolve at the same time the low-frequency peak and the slow convergence of impedance to zero at high frequencies.

CSR Instability Analytic Estimates

Here, we present semi-analytical estimations of the coherent-synchrotron-radiation instability for Diamond-II using scaling laws found in Ref. [4]. When an electron is moving on the closed orbit with a bend radius ρ between two parallel plates separated by $2\,h$ gap, the dimensionless threshold strength is defined by

$$(S_{\mathrm{CSR}})_{\mathrm{th}} = 0.5 + 0.12\,\Pi, \quad (1)$$

where the dimensionless shielding parameter is $\Pi = \sigma_z\sqrt{\rho/h^3}$ and σ_z is the bunch length. In Diamond-II, the dipole magnets have different bend radii; four DL-type magnets consisting of five pieces each, whilst antibends and DQ dipoles consist of one piece. We list in Tab. 1 only the minimum value of the threshold bunch current corresponding to the minimum bend radius for the DL-type magnets.

Table 1: Summary of CSR instability thresholds for different magnet types in Diamond-II with and without harmonic cavity

magnet	ρ_{min} [m]	Min[$(I_b)_{\mathrm{th}}$] [mA]	
		IDs closed	IDs with 3HC
DL type 1	14.0	2.1	10.49
DL type 2	15.12	2.12	10.63
DL type 3	15.12	2.12	10.63
DL type 4	14.0	2.1	10.49
Antibend	57.3	2.36	12.79
DQ	16.8	2.13	10.74

Longitudinal Plane

In this section, all transverse impedance and wake elements have been excluded from the tracking simulations.

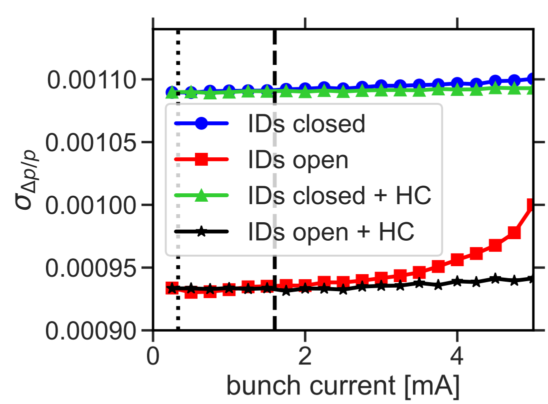

Figure 1: Microwave instability threshold determined by growth of the momentum spread with the bunch current.

In Fig. 1 and all figures below, the blue dots correspond to the case when IDs are closed, red squares to IDs open, green triangles and black stars to the cases when IDs are closed with the harmonic cavity and IDs are open with the harmonic cavity respectively. For reference, the bunch current for the standard filling pattern corresponds to 0.33 mA (0.6 nC, black dotted line). The bunch current for the hybrid filling

* dmitrii.rabusov@diamond.ac.uk

Content from this work may be used under the terms of the CC BY 4.0 licence (© 2024). Any distribution of this work must maintain attribution to the author(s), title of the work, publisher, and DOI.

ISBN: 978-3-95450-247-9 ISSN: 2673-5490 doi: 10.18429/JACoW-IPAC2024-MOPS33

pattern is 1.6 mA (3 nC, black dashed line). Microwave-instability (MW) thresholds correspond to 4.75 mA when IDs are closed, and 3 mA when IDs are open. The harmonic cavity further suppresses the MW instability (9 mA for Closed IDs, 4.75 mA for Open IDs).

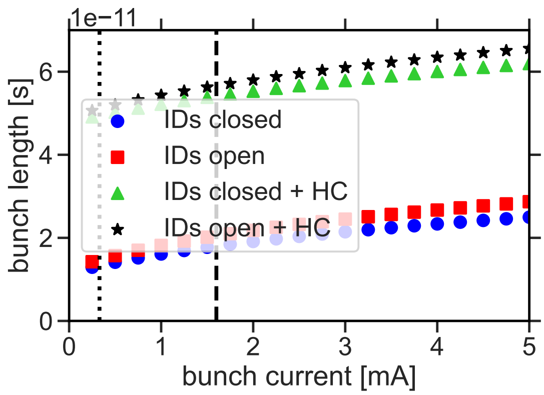

Figure 2: Bunch lengthening with increasing bunch current.

Figure 2 shows the equilibrium bunch length obtained in simulations with longitudinal wake fields. The bunch lengthening is nonlinear with bunch current.

Transverse Plane

Here, we include both longitudinal and transverse impedance and wake elements in the model. This allows head-tail thresholds to be estimated more accurately, since the additional charge-dependent bunch lengthening increases the impedance-safety margin in the transverse planes.

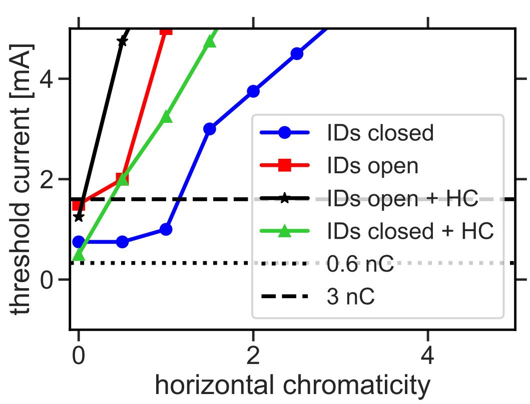

Figure 3: Head-tail threshold bunch current vs horizontal chromaticity.

Horizontal and vertical instabilities can be distinguished by disregarding vertical wake fields in horizontal-plane simulations and horizontal wake fields in vertical-plane simulations. Passive strategies for mitigating head-tail instabilities involve operating at higher chromaticity and/or elongating the bunch length using the harmonic cavity. Results shown in Fig. 3 indicate that $\xi_x > 1.5$ provides a factor-two safety margin against horizontal head-tail instabilities.

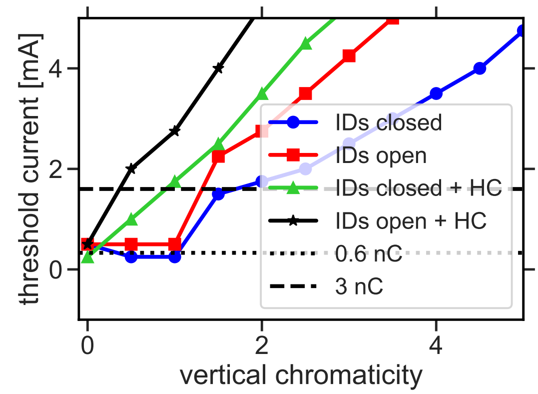

Figure 4: Head-tail threshold bunch current vs vertical chromaticity.

The gap h of the vacuum chamber is significantly smaller in the vertical plane, and the resistive-wall impedance is proportional to h^{-3}. Therefore, vertical head-tail instabilities are expected to be stronger, as shown in Fig. 4. It is found that $\xi_y > 1.5$ is required for stable operation for the hybrid-fill pattern, whilst $\xi_y > 3.5$ allows a factor-two safety margin.

Emittance Growth

This section presents the analysis of single-bunch instabilities in Diamond-II, focusing on emittance dilution caused by asymmetric components of the vacuum chamber. We tested two tracking models in Elegant with a lattice featuring asymmetric vacuum components. The first model consists of monopole and quadrupole wake elements distributed throughout the ring and transfer matrices between them to give the correct phase advances between elements. The second simplified model is a one-turn map with monopole and quadrupole wakes integrated throughout the ring and weighted by horizontal and vertical beta functions.

It was found that the simplified model with the integrated monopole and quadrupole components of the wake-field potential provides reasonable results with significantly reduced computational time. The results of particle tracking with the one-turn map illustrated in Fig. 5 show that emittance dilution in Diamond-II is expected to be negligible.

SELF-CONSISTENT SIMULATIONS WITH HARMONIC CAVITY

Due to the beam-loading effect, each bunch in the beam receives an effective potential with voltage and phase shifted from their nominal values for each cavity, thus, the flat-potential condition for the harmonic cavity cannot be applied for all bunches and for all currents. Consequently, the harmonic cavity provides unequal bunch lengthening throughout the beam. Diamond-II benefits from the 3rd harmonic cavity (3HC) in terms of higher instability thresholds

Content from this work may be used under the terms of the CC BY 4.0 licence (© 2024). Any distribution of this work must maintain attribution to the author(s), title of the work, publisher, and DOI.

15th International Particle Accelerator Conference,Nashville, TN JACoW Publishing
ISBN: 978-3-95450-247-9 ISSN: 2673-5490 doi: 10.18429/JACoW-IPAC2024-MOPS33

© Content from this work may be used under the terms of the CC BY 4.0 licence (© 2024). Any distribution of this work must maintain attribution to the author(s), title of the work, publisher, and DOI.

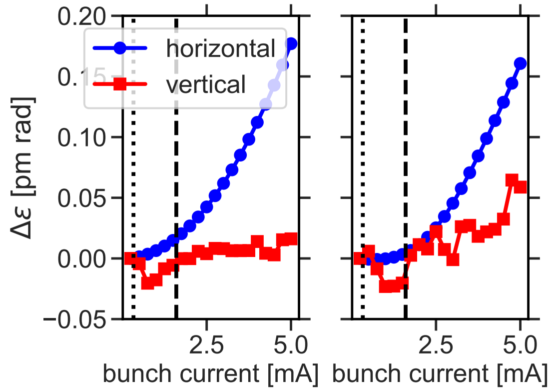

Figure 5: Emittance growth after 100 thousand turns due to monopole and quadrupole wake fields, IDs are closed (left), open (right).

and lifetime [5]. Therefore, beam loading might cause single-bunch instability thresholds to reduce for some bunches of the beam. However, single-bunch simulations require hundreds of thousands of macroparticles, and tracking with this resolution with the full beam is computationally challenging. Here we present a method for how to include beam loading in single-bunch simulations. As shown above and in Ref. [1], the most challenging case is for the timing bunch in hybrid-fill patterns when IDs are closed, especially in the vertical plane. We validate here the results shown in the previous section that were obtained using a simplified model with 3HC set to flat-potential conditions.

Beam Loading

We start with tracking the full beam but with reduced number of macroparticles per bunch, namely, 5 thousand macroparticles per bunch in the trains and 6-40 thousand macroparticles in the timing bunch. We use the beam corresponding to hybrid-fill patterns with varying timing-bunch charge from 1 nC to 5 nC. Also, we vary κ, the gap between the hybrid bunch and the trains in the hybrid-fill, as this requirement varies according to the needs of individual beam lines [5]. The results below correspond to κ = (10, 35, 75, 100) buckets. The main and harmonic cavities are modelled as *RFMODE* elements to extract the effective voltages and phases for both cavity types as seen by the timing bunch in simulations. Combining the results, we can find the scaling laws for cavity voltages and phases.

Single Bunch and Effective RF Parameters

Next, we can apply the effective RF voltages and phases found from the scaling laws, depending on the charge of the timing bunch and the gap between the trains in the hybrid-fill patterns, to the *RFCA* elements to simulate just the timing bunch, but now with a bunch distribution increased to 200 thousand macroparticles.

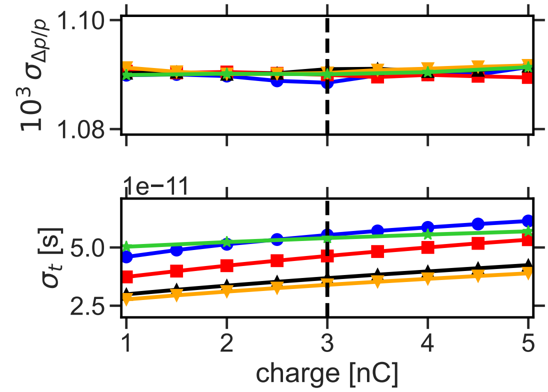

Figure 6: Momentum-spread (top) and bunch lengthening with bunch charge (bottom). The half gap between bunch trains, κ is 10 (blue dots), 35 (red squares), 75 (black triangles), 100 (orange triangles), and the results with the flat potential correspond to green stars.

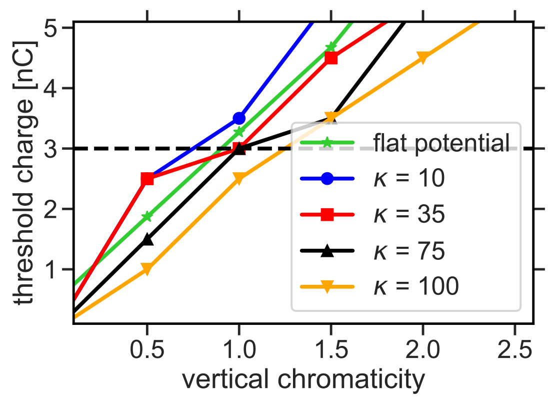

Figure 7: Vertical head-tail instability thresholds vs vertical chromaticity.

Results in Figs. 6 and 7 show that the flat-potential model provides reasonable results and the MW and the head-tail instabilities can be estimated even for κ = 100.

CONCLUSIONS

The results of this work include the updates to the MW and head-tail instabilities in Diamond-II. Chromaticity adjustment and a passive harmonic cavity are considered as mitigation measures. CSR instability threshold has been analytically estimated. Nominal bunch currents are below thresholds even without the harmonic cavity. Resulting emittance dilution due to monopole and quadrupole impedance is found to be negligible. Self-consistent simulations with hybrid bunch and the harmonic cavity show that the nominal timing-bunch charge is well below MW threshold and chromaticity above 1.5 is sufficient to mitigate transverse instabilities even for a half-gap of 100 buckets.

ISBN: 978-3-95450-247-9 ISSN: 2673-5490 doi: 10.18429/JACoW-IPAC2024-MOPS33

REFERENCES

[1] D. Rabusov, R. Fielder, and S. Wang, "Analysis of single-bunch instabilities for diamond-ii," in *Proc. IPAC'23*, Venice, Italy, 2023, pp. 3550–3553. doi:10.18429/JACoW-IPAC2023-WEPL184

[2] R. Fielder, D. Rabusov, and S. Wang, "Updates to the impedance database for the Diamond-II storage ring," presented at IPAC'24, Nashville, TN, USA, May 2024, paper THPC50, this conference.

[3] M. Borland, "Elegant: A flexible sdds-compliant code for accelerator simulation," 2000. doi:10.2172/761286

[4] K. L. F. Bane, Y. Cai, and G. Stupakov, "Threshold studies of the microwave instability in electron storage rings," *Phys. Rev. ST Accel. Beams*, vol. 13, p. 104 402, 10 2010. doi:10.1103/PhysRevSTAB.13.104402

[5] *Diamond-II Technical Design Report, Diamond Light Source*, https://www.diamond.ac.uk/Home/News/LatestNews/2022/14-10-22.html, Accessed: 2023-04-25.

Content from this work may be used under the terms of the CC BY 4.0 licence (© 2024). Any distribution of this work must maintain attribution to the author(s), title of the work, publisher, and DOI.